Facile microfluidic method for measuring the relaxation time of dilute polymer solution based on viscoelastic particle focusing

Yoonyoung Jung*, Tae Soup Shim*,**,†, and Ju Min Kim*,**,†

*Department of Energy Systems Research, Ajou University, Suwon 16499, Korea
**Department of Chemical Engineering, Ajou University, Suwon 16499, Korea

Abstract−The relaxation time of a viscoelastic fluid is an essential parameter for characterizing the degree of elasticity. However, measuring the relaxation time of dilute polymer solutions with low viscosity using conventional rotational rheometers remains challenging because of the low instrument sensitivity. In this study, we demonstrate an efficient microfluidic method for measuring the relaxation time of a dilute polymer solution by utilizing elasticity-driven lateral particle migration in a microchannel. First, the previous theoretical model was refined, based on the Oldroyd-B constitutive equation, in order to predict lateral particle migration in a viscoelastic fluid with constant shear viscosity, considering the inlet and finite particle size effects. This model was utilized to determine the relaxation times of dilute poly(ethylene oxide) (PEO) aqueous solutions. Direct comparison of the measured relaxation times with those obtained from Zimm theory verified the reliability of the proposed method. The current approach is expected to be useful in characterizing the relaxation times of a wide range of polymer solutions.

Keywords: Relaxation Time, Dilute Polymer Solution, Viscoelasticity, Microchannel, Lateral Particle Migration

INTRODUCTION

Viscoelastic non-Newtonian fluids, including polymer solutions, have been extensively used in a wide range of daily and industrial applications [1,2]. It is well known that polymer solutions containing long and flexible polymer molecules dissolved in a solvent have significant viscoelastic properties even at very low polymer concentrations [1]. Recent work has demonstrated that the viscoelasticity of deoxyribonucleic acid (DNA) solutions is significant, even when the DNA concentration is extremely low (only a few ppm) [3]. Measuring the relaxation time is critical for characterizing the viscoelastic properties of polymer solutions [1,2]. However, determining the relaxation time of a dilute polymer solution with low viscosity using standard rheometry techniques such as commercial rotational rheometers remains challenging [4,5].

Many studies have been devoted to measuring the relaxation time of dilute polymer solutions using techniques such as capillary break-up rheometry (CaBER) [6] and microfluidic technologies [4,7,8]. However, commercialized CaBER can be applied to viscoelastic fluids with a relaxation time greater than a millisecond [6], and it was reported that the relaxation time measured using CaBER is not consistent with that of conventional rotational rheometry, which necessitates the careful use of the CaBER-based relaxation time [9]. Microfluidics-based approaches for measuring the rheological properties of complex fluids have been also proposed, since such methods require a small sample volume and the fluid flow can be precisely controlled in microfluidic channels [4,7,10-13].

Lateral particle migration occurs owing to inertial forces in a Newtonian fluid [14], which can also be induced by imbalanced normal stress differences in the pressure-driven viscoelastic flow even at negligibly small Reynolds number (Re) [15-17]. The particles under inertial flow are annularly accumulated at the location of 0.6 times the tube radius (R) in a circular microchannel [14], while particle focusing occurs along the channel centerline in viscoelastic fluids with constant shear viscosity, such as dilute polymer solutions [18]. Normal stress difference-driven particle focusing along the centerline in microchannels has been found in very weakly elastic complex fluids, such as extremely dilute DNA solutions and nanoparticle colloidal dispersions [3,13]. Therefore, particle focusing along the microchannel centerline has been shown to be a method of confirming that the particle-suspending medium is a viscoelastic fluid [13]. Recent studies have demonstrated that viscoelasticity-driven particle focusing can be used to characterize the relaxation times of complex fluids with short relaxation times, such as dilute polymer solutions and colloidal dispersions [7,8,13]. However, the existing methods either require extensive numerical simulation results and complicated particle tracking methods [7] or are based on the assumption that a viscoelastic fluid has very weak elasticity [13].

In this study, we refined a previous theoretical model [3], based on the Oldroyd-B constitutive equation, in order to predict the outermost locations of particles resulting from lateral particle migration in a viscoelastic fluid at a specific distance from the channel inlet, taking into account the inlet and non-negligible particle size effects [19]. The updated model was used to determine the relaxation times of dilute poly(ethylene oxide) (PEO) solutions simply by fitting the experimental data without extensive numerical simulation and particle tracking. The empirical parameter in the theoretical model was determined using the relaxation time of a PEO

solution, which can be measured using the existing method [4]. The developed method was demonstrated to be reliable by comparing the measured relaxation times with those from Zimm theory, which predicts the relaxation time of a dilute polymer solution.

THEORETICAL BACKGROUND

Previous theoretical studies [15,17] have predicted that lateral particle migration, occurring in the pressure-driven flow of a viscoelastic fluid [20], is induced by imbalanced normal stress differences. Micron-sized particles suspended in a viscoelastic fluid with constant shear viscosity (or Boger fluid [21]) laterally migrate toward the channel centerline and form a focused stream along the centerline in a circular microchannel [3,18]. In contrast, particles may migrate toward the channel wall in shear-thinning fluids [18]. Viscoelastic particle migration has also been predicted using direct numerical simulations based on viscoelastic constitutive equations [20].

As demonstrated hereinafter, the shear viscosity of the dilute PEO solutions considered in this study was constant with little variation with respect to the shear rate. Therefore, the dilute PEO solutions used in this study are Boger fluids, which can be modeled using the Oldroyd-B constitutive equation [21]. Viscoelastic particle migration and focusing are induced by the first normal stress difference (N_1) in a Boger fluid [17]. The second normal stress difference (N_2) is regarded as negligibly small in the case of Boger fluids because the magnitude of the first normal stress differential (N_1) is substantially larger than that of N_2 [17,21]. In the viscoelastic pressure-driven microchannel flow in a circular tube, the radial particle distribution resulting from lateral particle migration, which is induced by non-uniform N_1, can be predicted at a certain distance ($\Delta z = z_b - z_a$) from channel location z_a as follows:

$$2\ln\frac{r_b}{r_a} + \left(\frac{r_a}{R}\right)^2 - \left(\frac{r_b}{R}\right)^2 = \alpha_p \frac{\Delta z}{R} \frac{\eta - \eta_s}{\eta} Wi\left(\frac{a}{R}\right)^2 \qquad (1)$$

where r_b and r_a are the outermost locations at distances z_b and z_a from the channel inlet, respectively [3]. The symbols η and η_s denote the shear viscosities of the polymer solution and the corresponding solvent, respectively; a is the radius of the particles suspended in the polymer solution, and the empirical parameter α_p is determined by analyzing a viscoelastic fluid with a known relaxation time. Wi is the Weissenberg number, defined as $Wi \equiv \lambda \frac{\langle u_z \rangle}{R}$ (λ: relaxation time of the polymer solution, $\langle u_z \rangle$: average velocity in the channel cross-section, R: channel radius). However, the channel inlet effects and particle size must be considered [19]. Therefore, the outermost location (r_i) of the particles is defined as $r_i = \alpha R$ ($0 \leq \alpha < 1$) at the channel inlet. Consequently, Eq. (1) is changed to the following form:

$$2\ln\frac{r_p}{R} + 1 - \left(\frac{r_p}{R}\right)^2 = \alpha_p \frac{\Delta z}{R} \frac{\eta - \eta_s}{\eta} Wi\left(\frac{a}{R}\right)^2 + Y_P \qquad (2)$$

where the left-hand side of the above equation is defined as the "focusing index," which provides a quantitative measure of particle focusing when the particles travel a distance Δz from the channel inlet [3]. In Eq. (2), Y_P represents the uncertainty term arising from

the inlet and non-negligible particle-size effects, as mentioned above.

EXPERIMENTAL

1. Materials

Aqueous solutions of glycerin (22 and 60 wt%; Sigma-Aldrich) were used as Newtonian fluids, and were also used as solvents for the PEO solutions. Viscoelastic polymer solutions were prepared by dissolving PEO with various molecular weights (Sigma-Aldrich, M_w=300, 1,000, 2,000, and 4,000 kg/mol) in 22 or 60 wt% aqueous glycerin solution. The PEO concentrations (c: 1472, 673, 429, and 273 ppm) in the 22 wt% glycerin solution were determined to match the halves of the overlapping concentrations ($c^* = \frac{0.77}{[\eta]}$ [22]) of PEO with molecular weights of 300, 1,000, 2,000, and 4,000 kg/mol, where $[\eta]$ denotes the intrinsic viscosity. Therefore, all these polymer solutions are in the dilute regime [23,24]. Aqueous PEO solutions (100, 200, 429, 600, 900, 1,200, and 1,500 ppm) were prepared from PEO with 2,000 kg/mol molecular weight (2 M) in 22 wt% aqueous glycerin solution to investigate the effects of the PEO concentration on the relaxation time. A 500 ppm dilution of 2 M PEO solution in 60 wt% aqueous glycerin solution was also prepared for the experiment to measure the relaxation time with N_1. In this work, 0.01 wt% polystyrene (PS) beads (6 μm diameter, Polysciences) were added to the PEO solutions, where the densities of the PS and PEO solutions were matched to prevent particle sedimentation in the microchannel experiments for lateral particle migration [25]. In addition, 0.01 wt% nonionic surfactant (TWEEN 20, Sigma-Aldrich) was added to the PEO solutions to minimize particle-particle adhesion.

The shear viscosity of all the solutions was measured at 20 °C with a rotational rheometer (AR-G2, TA Instruments) having a cone and plate geometry (diameter: 60 mm, angle: 1°). The shear viscosities of the 22 and 60 wt% glycerin aqueous solutions were measured to be 1.91 and 10.93 cP, respectively. The Zimm relaxation time (λ_z) of the PEO aqueous solutions was determined according to previous studies [23,25,26] as follows:

$$\lambda_z = F\frac{[\eta]M_w\eta_s}{N_A k_B T} \qquad (3)$$

where the pre-factor, F, is 0.463, which is determined by the solvent quality [26]. N_A is Avogadro's constant, k_B is Boltzmann's constant, and T is the absolute temperature. The intrinsic viscosity ($[\eta]$) of the PEO solution in the 22 wt% glycerin aqueous solution was determined using the relationship $[\eta] = 0.072M_w^{0.65}$ [23]. However, for the 2 M PEO solution in 60 wt% aqueous glycerin, the intrinsic viscosity of 582 cm^3/g, which was separately measured [27], was used because the solvent quality is significantly different from that of the 22 wt% glycerin solution. Table 1 lists the estimated intrinsic viscosities and Zimm relaxation times of the PEO solutions considered in this study.

2. Fabrication of Microchannel

The microchannels for the lateral particle migration experiments in the PEO solutions were fabricated using almost the same method described in our previous work [3] using a straight cylindrical microtube (PEEKsil Tubing, IDEX Health & Science; 50 μm inner diameter and 5 cm length). Briefly, the polymer layer covering the

Table 1. Intrinsic viscosities and Zimm relaxation times of solutions of poly(ethylene oxide) with different molecular weights

Molecular weight (kg/mol)	Intrinsic viscosity (cm³/g)	c^* (ppm)	c (ppm)	Zimm relaxation time (ms)
3×10^2	2.61×10^2	2,944	1,472	0.028
1×10^3	5.72×10^2	1,346	673	0.208
2×10^3	8.97×10^2	858	429	0.651
4×10^3	1.41×10^3	547	273	2.044

silica capillary tube was burned off using an alcohol lamp to observe the particles flowing inside the circular tube [3]. The capillary tube was placed between two cover glasses filled with glycerin to minimize light scattering at the exposed silica capillary outer wall. Before the lateral particle migration experiments, TWEEN 20 aqueous solution (0.1 vol%) was flowed through the capillary tube at a rate of 15 μl/h for 30 min to prevent the particles from sticking to the inner wall of the channel.
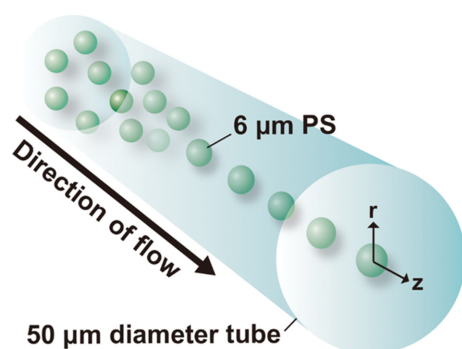
3. Lateral Particle Migration Experiments and Image Acquisition

Lateral particle migration in the PEO aqueous solutions was observed by using an inverted microscope (IX-71, Olympus), and the flow rate was controlled with a syringe pump (11 Plus, Harvard Apparatus). The images were captured at 60 frames per second with a 1/8,000 s exposure time. From the acquired images, the locations of the particles were determined by following a previously described approach [25]. The outermost locations (r_p's) of the particles (refer to the theoretical background for the definition of r_p) were obtained at downstream locations of 1, 2, 3, and 4 cm from the channel inlet by applying the $\langle \mathrm{Max} - \mathrm{Min} \rangle$ criterion explained in our previous work [3].
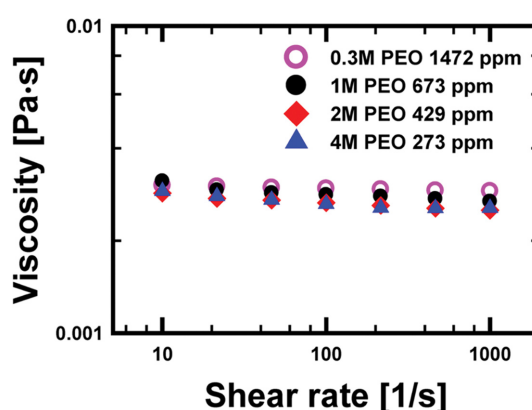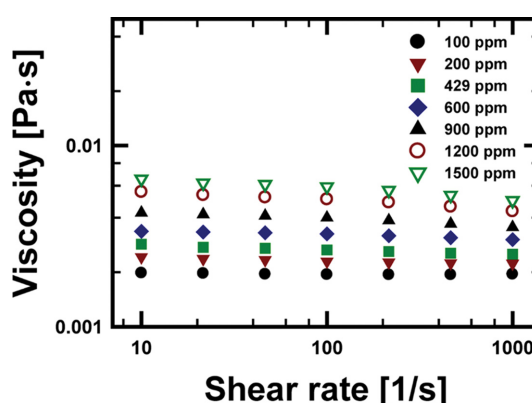
RESULTS AND DISCUSSION

1. Measurement of Relaxation Time Based on the First Normal Stress Difference and Determination of Empirical Parameter α_p

The relaxation time of a dilute polymer solution containing PS beads with a diameter of 6 μm was determined based on the lateral particle migration and focusing phenomenon, as shown in Fig. 1. Lateral particle migration occurred when the PS bead-laden polymer solution flowed through the cylindrical capillary tube with

an inner diameter of 50 μm. As shown in Figs. 2 and 3, the shear viscosities of the polymer solutions did not change significantly as the shear rate increased. Therefore, it was assumed that the PEO solutions were Boger fluids, which can be modeled using the Old-

Fig. 2. Viscosities of aqueous poly(ethylene oxide) solutions with various molecular weights (Mw=300, 1,000, 2,000, 4,000 kg/mol) in 22 wt% glycerin aqueous solution under the condition that the ratio of polymer concentration to overlapping concentration is set to 0.5. The viscosity was measured at 20 °C using a rotational rheometer (AR-G2, TA instruments) with a cone and plate geometry (diameter: 60 mm, angle: 1°).

Fig. 3. Change in viscosity of 2,000 kg/mol poly(ethylene oxide) solution in 22 wt% glycerin aqueous solution according to the polymer concentration (c=100, 200, 429, 600, 900, 1,200, and 1,500 ppm). Viscosity was measured at 20 °C using a rotational rheometer (AR-G2, TA instruments) with a cone and plate geometry (diameter: 60 mm, angle: 1°). The viscosity data of 429 ppm solution in Fig. 2 are re-plotted here for comparative purposes.

Fig. 1. Schematic of viscoelastic particle focusing-based rheometry setup.
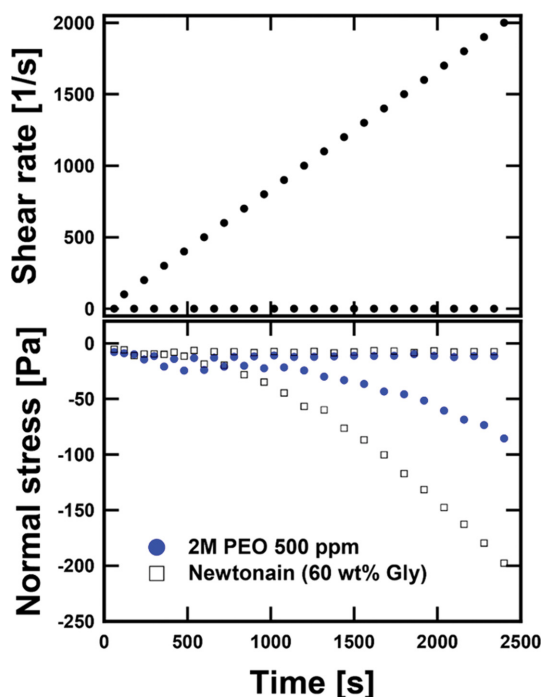
Fig. 4. Protocol for ramping the shear rate up to measure the first normal stress difference using a rotational rheometer (AR-G2, TA Instruments) with a cone and plate geometry (diameter: 60 mm, angle: 1°) (upper panel), and measured normal stress difference values for 500 ppm 2 M PEO solution in 60 wt% glycerin aqueous solution (viscoelastic), and 60 wt% glycerin aqueous solution (Newtonian) (lower panel).
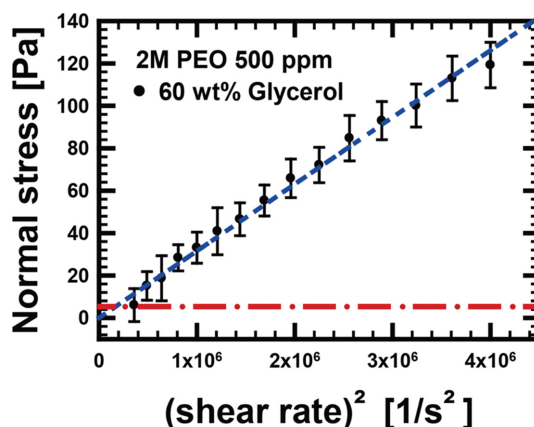

Fig. 5. First normal stress difference of 500 ppm 2 M PEO solution in 60 wt% glycerin aqueous solution as a function of the square of shear rate. The horizontal dash-dot line indicates three times the measurement limit, where the measured values were discarded below the limit.
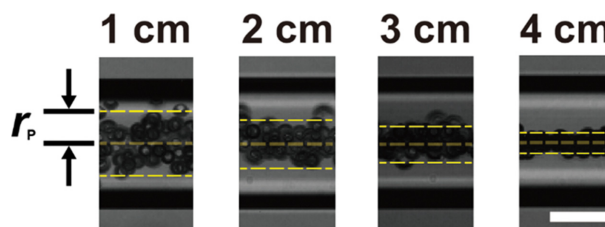

Fig. 6. Particle distribution in the microchannel at a flow rate of 20 μl/h according to the distance from the inlet (images were acquired using a z-projection with 'min intensity' mode of ImageJ software). The scale bar denotes 25 μm.

royd-B constitutive equation. The relaxation times of the PEO solutions were determined using Eq. (2); however, the equation contains an empirical parameter α_p that must be determined using a viscoelastic fluid with a known relaxation time. To determine the empirical parameter α_p, 500 ppm of a 2 M PEO solution in 60 wt% aqueous glycerin was selected, for which the first normal stress difference N_1 could be measured with a rotational rheometer (AR-G2, TA Instruments) having a cone and plate geometry (60 mm diameter, 1° angle). However, when a rotational rheometer with cone and plate geometry is used to measure N_1, the measurement may be subject to inertial and drift effects that should be corrected [4,5,28]. A protocol for ramping up the shear rate was employed to alleviate the inertial and drift effects, as shown in the upper panel of Fig. 4, based on the previous study [28]. The shear rate was increased in the following manner: the shear rate was initially maintained at 0.01 s^{-1} for 60 s, increased to 100 s^{-1} for 60 s, reset to 0.01 s^{-1} for 60 s, then increased to 200 s^{-1} for 60 s, and so on until the shear rate reached 2,000 s^{-1}. The first 20 s at each shear rate was regarded as the time it took to reach equilibrium, and the average values of the data for the next 40 s were obtained, which are presented in the bottom panel of Fig. 4. As shown in Fig. 5, the N_1 data for the PEO solution were corrected by considering the errors arising from the drift and inertial effects using those of the Newtonian solvent (60 wt% glycerol aqueous solution). From Fig. 5, the relaxation time (λ) of the PEO solution was determined to be 3.48 ms by applying Eq. (4) [1,4]:

$$\lambda = \frac{\Psi_1}{2\eta_p(\dot{\gamma})} = \frac{\Psi_1}{2[\eta(\dot{\gamma}) - \eta_s(\dot{\gamma})]} \qquad (4)$$

where Ψ_1 denotes the first normal stress difference coefficient defined as $\Psi_1 = N_1(\dot{\gamma})/\dot{\gamma}^2$. The relaxation time of the 500 ppm 2 M PEO solution in 22 wt% aqueous glycerin was found to be 0.72 ms using the relationship $\lambda = A\eta_s^{0.9}$ [4].

Lateral particle migration experiments in 429 ppm 2 M PEO (Mw=2,000 kg/mol) solution in a 22 wt% glycerin aqueous solution were performed at flow rates of 10 μl/h and 20 μl/h, as shown in Fig. 6. The outermost location (r_p) was determined by following the procedures in the experimental section, as shown in Fig. 7, where $\alpha_p = -6.07 \pm 1.11$. Note that the relaxation time of the 429 ppm PEO solution is assumed to be the same as that of the 500 ppm PEO solution because the relaxation time is a very weak function of the polymer concentration below the overlapping concentration [29], which is also validated in the following section.

2. Determination of Relaxation Time of PEO Solution Based on Viscoelastic Particle Focusing

The empirical parameter determined in the previous section was substituted into Eq. (2), which was used to obtain the relaxation times of the 2 M PEO solutions in the 22 wt% aqueous glycerin solution with various PEO concentrations, as shown in Fig. 8. The relaxation times did not notably change up to $c \approx c^*$, and were close
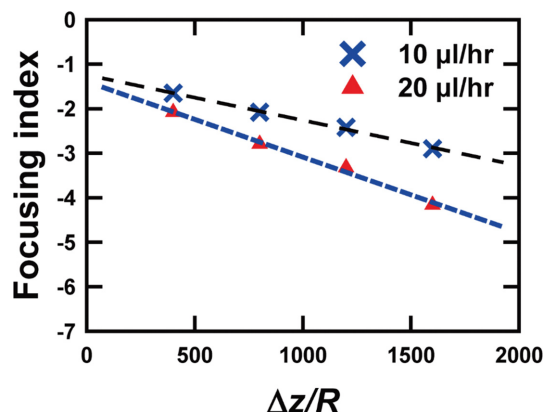
Fig. 7. "Focusing index" versus normalized traveling distance of particles ($\Delta z/R$). "Focusing index" is represented by $2\ln\dfrac{r_p}{R}+1-\left(\dfrac{r_p}{R}\right)^2$ in Eq. (2).

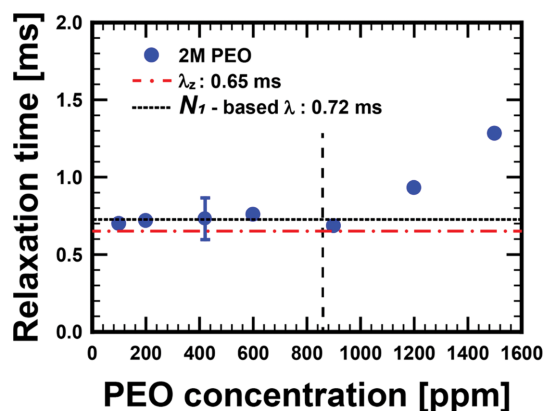**Fig. 8.** Viscoelastic particle focusing was used to measure relaxation time as a function of PEO (Mw=2,000 kg/mol) concentration in 22 wt% glycerin aqueous solution. The vertical line denotes the overlapping concentration. The horizontal dash-dot line corresponds to the Zimm relaxation time, and the dotted line is the relaxation time obtained with the first normal stress difference.

to the Zimm relaxation time (horizontal dash-dotted line). However, the relaxation time started to deviate significantly from the Zimm relaxation time above $c=c^*$. In the figure, the vertical line corresponds to the overlapping concentration (c^*=858 ppm) and the dotted horizontal line denotes the relaxation time obtained with the first normal stress difference, as described in the previous section. The current findings, which show that the measured relaxation times in the dilute polymer solution regime ($c<c^*$) match the Zimm relaxation time, are consistent with polymer theory [24]. However, we could not confirm the progressive increase in the relaxation time around $c\approx c^*$ that was observed in a previous study [29], necessitating further studies with more experimental data to confirm the increase in the relaxation time around $c\approx c^*$. The significant deviation in the relaxation time from the Zimm relaxation time above $c>c^*$ originates from the polymer-polymer interaction, which is also consistent with the existing polymer physics theories
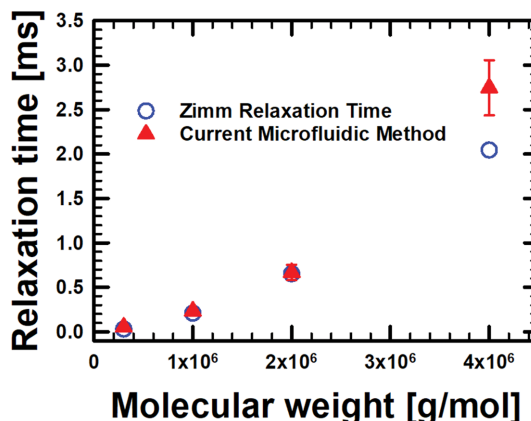
Fig. 9. Relaxation time as a function of PEO molecular weight in 22 wt% glycerin aqueous solution. The ratio of the polymer concentration to the overlapping concentration (c/c^*) was set to 0.5 for all the cases. Note that the relaxation time of 2 M PEO solution in Fig. 8 is added here for comparative purposes.

[24,29].

Fig. 9 shows the relaxation times of the PEO solutions with various molecular weights in 22 wt% glycerin aqueous solutions in the dilute polymer solution regime (c/c^*=0.5). The relaxation times for all molecular weights were comparable to the Zimm relaxation time for each molecular weight. The current results demonstrate that the microfluidic method used in this study can be applied to measure the relaxation times of dilute PEO solutions. Note that at all the flow conditions considered in this study, the Reynolds numbers were below unity, which precludes significant inertia-induced particle migration. In future work, we intend to investigate whether the current method can be applied to other polymer systems in a dilute regime.

CONCLUSION

A simple method of measuring the relaxation time of polymer solutions with low viscosity based on viscoelastic lateral particle migration and focusing in a microchannel was presented. A previous theoretical model was slightly refined, based on the Oldroyd-B model, and used to predict the lateral particle migration in viscoelastic fluids by considering the inlet and non-negligible particle size effects. First, the relaxation time of a 500 ppm 2 M PEO solution in a viscous 60 wt% glycerin medium was measured based on the first normal stress difference data. This relaxation time was then used to estimate the relaxation time of the 500 ppm 2 M PEO solution in the 22 wt% glycerin aqueous solution. The empirical parameter, which appears in the theoretical model, was determined using a 500 ppm 2 M PEO solution in a 22 wt% glycerin aqueous solution with a known relaxation time. The relaxation times measured as a function of the PEO concentration are consistent with the existing theories: the measured relaxation times, which are close to the Zimm relaxation time, did not change significantly up to $c\approx c^*$, but significantly deviated from the Zimm relaxation time above $c\approx c^*$. The dependence of the relaxation time on the PEO molecular weight in the dilute regime was also investigated, demon-

strating a monotonic increase with increasing PEO molecular weight. All the measured relaxation times of the PEO solutions with different molecular weights are comparable to the Zimm relaxation times, which demonstrates the reliability of this work. We expect that the proposed method can be widely used to measure the relaxation times of dilute polymer solutions.

ACKNOWLEDGEMENTS

REFERENCES

1. R. B. Bird, R. C. Armstrong and O. Hassager, *Dynamics of polymeric liquids*, Wiley Interscience, New York (1987).
2. R. G. Larson, *The structure and rheology of complex fluids*, Oxford University Press, New York (1999).
3. K. Kang, S. S. Lee, K. Hyun, S. J. Lee and J. M. Kim, *Nat. Commun.*, **4**, 2567 (2013).
4. J. Zilz, C. Schafer, C. Wagner, R. J. Poole, M. A. Alves and A. Lindner, *Lab Chip*, **14**, 351 (2014).
5. C. W. Macosko, *Rheology: principles, measurements, and applications*, Wiley-VCH (1994).
6. L. E. Rodd, T. P. Scott, J. J. Cooper-White and G. H. McKinley, *Appl. Rheol.*, **15**, 12 (2004).
7. F. Del Giudice, G. D'Avino, F. Greco, I. De Santo, P. A. Netti and P. L. Maffettone, *Lab Chip*, **15**, 783 (2015).
8. F. D. Giudice, S. J. Haward and A. Q. Shen, *J. Rheol.*, **61**, 327 (2017).
9. C. Clasen, J. P. Plog, W.-M. Kulicke, M. Owens, C. Macosko, L. E. Scriven, M. Verani and G. H. McKinley, *J. Rheol.*, **50**, 849 (2006).
10. J. M. Kim, *Korean J. Chem. Eng.*, **32**, 2406 (2015).
11. D. Y. Kim and J. M. Kim, *Korean J. Chem. Eng.*, **36**, 837 (2019).
12. A. Shiriny, M. Bayareh and A. A. Nadooshan, *Korean J. Chem. Eng.*, **38**, 1686 (2021).
13. B. Kim, S. S. Lee, T. H. Yoo, S. Kim, S. Y. Kim, S.-H. Choi and J. M. Kim, *Sci. Adv.*, **5**, eaav4819 (2019).
14. É. Guazzelli and J. F. Morris, *A physical introduction to suspension dynamics*, Cambridge University Press, Cambridge (2012).
15. B. P. Ho and L. G. Leal, *J. Fluid Mech.*, **76**, 783 (1976).
16. A. Karnis, S. G. Mason and H. L. Goldsmith, *Nature*, **200**, 159 (1963).
17. A. M. Leshansky, A. Bransky, N. Korin and U. Dinnar, *Phys. Rev. Lett.*, **98**, 234501 (2007).
18. G. D'Avino, G. Romeo, M. M. Villone, F. Greco, P. A. Netti and P. L. Maffettone, *Lab Chip*, **12**, 1638 (2012).
19. G. Romeo, G. D'Avino, F. Greco, P. A. Netti and P. L. Maffettone, *Lab Chip*, **13**, 2802 (2013).
20. G. D'Avino, F. Greco and P. L. Maffettone, *Annu. Rev. Fluid Mech.*, **49**, 341 (2017).
21. D. F. James, *Annu. Rev. Fluid Mech.*, **41**, 129 (2009).
22. W. W. Graessley, *Polymer*, **21**, 258 (1980).
23. V. Tirtaatmadja, G. H. McKinley and J. J. Cooper-White, *Phys. Fluids*, **18**, 043101 (2006).
24. M. Rubinstein and R. H. Colby, *Polymer physics*, Oxford University Press, Oxford (2003).
25. S. Yang, J. Y. Kim, S. J. Lee, S. S. Lee and J. M. Kim, *Lab Chip*, **11**, 266 (2011).
26. L. E. Rodd, T. P. Scott, D. V. Boger, J. J. Cooper-White and G. H. McKinley, *J. Non-Newton. Fluid Mech.*, **129**, 1 (2005).
27. L. E. Rodd, J. J. Cooper-White, D. V. Boger and G. H. McKinley, *J. Non-Newton. Fluid Mech.*, **143**, 170 (2007).
28. L. Casanellas, M. A. Alves, R. J. Poole, S. Lerouge and A. Lindner, *Soft Matter*, **12**, 6167 (2016).
29. Y. G. Liu, Y. G. Jun and V. Steinberg, *J. Rheol.*, **53**, 1069 (2009).